

# Water Resources Research®

## RESEARCH ARTICLE

10.1029/2023WR034889

# Seasonal Early Warning of Impacts of Harmful Algal Blooms on Farmed Shellfish in Coastal Waters of Scotland



### Key Points:

- We present a new statistical approach for seasonal predictions of toxic *Dinophysis* species blooms in two regions of Scotland
- Results indicate a link between low winter-spring sea surface temperatures and high summer toxin concentrations in shellfish samples
- We demonstrate improved early warnings of harmful summer blooms using the first 120 days of sea surface temperature measurements each year

### Supporting Information:

Supporting Information may be found in the online version of this article.

### Correspondence to:

O. Stoner,  
oliver.stoner@glasgow.ac.uk

### Citation:

Stoner, O., Economou, T., & Brown, A. R. (2024). Seasonal early warning of impacts of harmful algal blooms on farmed shellfish in coastal waters of Scotland. *Water Resources Research*, 60, e2023WR034889. <https://doi.org/10.1029/2023WR034889>

Received 17 MAR 2023




Accepted 21 AUG 2024

### Author Contributions:

**Conceptualization:** O. Stoner, T. Economou, A. R. Brown  
**Data curation:** A. R. Brown  
**Formal analysis:** O. Stoner  
**Funding acquisition:** O. Stoner, A. R. Brown  
**Investigation:** O. Stoner  
**Methodology:** O. Stoner, T. Economou, A. R. Brown  
**Project administration:** O. Stoner, A. R. Brown  
**Software:** O. Stoner  
**Validation:** O. Stoner  
**Visualization:** O. Stoner

© 2024. The Author(s). *Water Resources Research* published by Wiley Periodicals LLC on behalf of American Geophysical Union.

This is an open access article under the terms of the [Creative Commons Attribution License](https://creativecommons.org/licenses/by/4.0/), which permits use, distribution and reproduction in any medium, provided the original work is properly cited.

O. Stoner<sup>1</sup> , T. Economou<sup>2,3</sup> , and A. R. Brown<sup>4</sup> 

<sup>1</sup>School of Mathematics and Statistics, University of Glasgow, Glasgow, UK, <sup>2</sup>Climate and Atmospheric Research Centre, The Cyprus Institute, Nicosia, Cyprus, <sup>3</sup>Department of Mathematics and Statistics, University of Exeter, Exeter, UK,

<sup>4</sup>Department of Biosciences, University of Exeter, Exeter, UK

**Abstract** Harmful Algal Blooms (HABs) can produce phycotoxins that accumulate in shellfish and subsequently poison aquatic predators and human consumers, potentially causing significant economic impacts to the shellfish aquaculture industry. HAB events are challenging to foresee as they are driven by complex inter-annual and seasonal changes in physical, chemical and biological factors. Accounting for these environmental drivers and their interactions in statistical models allows for the development of HAB early warning systems. Typically, these have a forecasting horizon of 1–2 weeks, allowing shellfish businesses and regulators to increase monitoring intensity and take evasive action, including harvesting suspensions to protect consumer health. However, there is critical need for longer-term predictions of risk, to enable more proactive mitigation, business planning, harvest scheduling and supply chain management. We present a statistical framework for providing seasonal-scale early warnings of the occurrence and impacts of *Dinophysis spp.* HABs on shellfish aquaculture in Scotland, UK. We use penalized smooth functions of winter-spring daily sea surface temperature to predict the severity and impact of ensuing summer blooms, including the percentage of toxicity measurements exceeding the harvesting closure threshold, as well as the anticipated start, end, and overall duration of closures. We illustrate the application of this framework to two Scottish aquaculture regions: One with a high spatial concentration of harvesting sites (Shetland) and one with more dispersed sites (West Scotland and the Hebrides). Through a comprehensive yearly prediction experiment, we demonstrate considerable skill in predicting the impact of unseen HAB seasons at a regional level.

## 1. Introduction

Harmful Algal Blooms (HABs) are frequently encountered throughout the world's coastal and shelf seas, and have been shown to asphyxiate or intoxicate marine life and impact upon marine aquaculture (mariculture) by causing fish kills or by contaminating seafood (Belin et al., 2021; Glibert et al., 2014; Hallegraef et al., 2021; Trainer et al., 2020; Weisberg et al., 2019; Wells et al., 2020). Moreover, the accumulation of algal toxins (phycotoxins) in filter feeding shellfish is a major threat to human health (Berdalet et al., 2016; Manfrin et al., 2012; Mardones et al., 2020). Toxins produced by HABs are associated with several shellfish poisoning syndromes, including Diarrhetic Shellfish Poisoning (DSP) (Manfrin et al., 2012; Mardones et al., 2020)—which is reported frequently in Europe (Mardones et al., 2020)—and generally involve dinoflagellate algae from the genus *Dinophysis* (Reguera et al., 2014). *Dinophysis* species are among the most problematic for shellfish farming/harvesting in Scotland and elsewhere in NW Europe. *D. acuta* and *D. acuminata* are known to produce lipophilic phycotoxins (okadaic acid (OA) and analogs dinophysistoxin-1 (DTX1) and dinophysistoxin-2 (DTX2), which are heat stable and unaffected by cooking (Reguera et al., 2014). When total *Dinophysis* toxins concentrations in shellfish exceed a safe threshold (160 µg OA equivalents/kg shellfish flesh), shellfish harvesting closures are imposed to safeguard the health of human consumers (European Commission, 2004a). In some European countries, including the UK, Spain, Portugal, Norway and Sweden, shellfish harvesting closures have lasted as long as 10 months (Berdalet et al., 2016).

The overall annual economic impact of HABs on shellfish mariculture production in Europe, including closures driven by toxic species such as *Dinophysis spp.*, has been estimated to be €0.95 billion (Hoagland & Scatista, 2006). This is not dissimilar from total annual shellfish sales (€1.134 billion), which represent ~50% of European aquaculture production, and approximately 8% of the world total shellfish production (STECF, 2018).

Occurrences and impacts of HABs vary considerably across local and regional scales, while being particularly severe in remote coastal communities and economies that almost entirely rely on shellfish farming (Mardones

**Writing – original draft:** O. Stoner,  
T. Economou, A. R. Brown  
**Writing – review & editing:** O. Stoner,  
T. Economou, A. R. Brown

et al., 2020). This situation is typical of many shellfish farming locations across Europe, but is particularly evident in Scotland (Gianella et al., 2021). The bulk of Scottish shellfish farming (mainly blue mussels, Pacific oysters and edible cockles) comprises about 200 small family businesses, which are vital to the economies of remote rural locations of the Scottish Highlands and Islands (Highlands and Islands Enterprise, Marine Scotland, 2017). There, prolonged shellfish harvesting closures are frequently caused by *D. acuminata* and *D. acuta* (Bresnan et al., 2021; Swan et al., 2018; Whyte et al., 2014). Resulting annual lost shellfish sales are estimated at £1.37 million/year (in 2015 currency), or ~15% of national annual industry turnover (Martino et al., 2020).

In this article we propose and evaluate a statistical framework for predicting seasonal characteristics of HAB severity, which could inform an Early Warning System (EWS) for the Scottish mariculture industry. In Section 2, we discuss existing efforts to monitor and predict *Dinophysis* HAB impacts and investigate potential links between winter-spring sea surface temperature and summer HABs. In Section 3, we describe our proposed framework for modeling toxin concentrations in shellfish, based on environmental factors, and explain how this can be linked to four seasonal measures of HAB severity and timing at a regional level. In Section 4, we apply this framework to regulatory data from two regions in Scotland separately—one where harvesting sites are more spatially concentrated (Shetland Islands) and one where they are spread out over a much larger area (West of Scotland)—and discuss out-of-sample prediction performance. Finally, in Section 5 we critically evaluate the suitability and benefits of our approach for development into a real-world seasonal EWS, and discuss avenues for further refinement or adaptation for shorter-term forecasting.

## 2. Background

### 2.1. Official Control Monitoring Data

“Official Control” monitoring of HABs at shellfish mariculture production sites in Europe involves regular weekly or bi-weekly in situ sampling and microscopic quantification of HAB species abundance in water and subsequent chemical analysis of phycotoxins in shellfish flesh (European Commission, 2004a, 2004b, 2004c). Monitoring in Scotland is carried out by Food Standards Scotland (Food Standards Scotland, 2022) and historical biotoxin data are freely available from Scotland's Aquaculture Website (Scotland's Aquaculture, 2022). Official Control monitoring quantifies both *Dinophysis* spp. abundance and OA toxin levels, as well as a range of other HAB species and associated toxins that can accumulate to harmful levels in shellfish. For example, another dinoflagellate *Prorocentrum lima* may be detected and is known to produce OA toxins (Bresnan, 2003). The data used here span March 2009–February 2022 and 122 harvesting locations. Figure 1 shows the 35 harvesting locations we include in the final analysis. Regular sampling and analysis can usually prevent the harvesting and consumption of shellfish containing harmful levels of phycotoxins. However, since this approach is retrospective, some poisonings may occur before harvested shellfish can be recalled from the market, and it cannot provide direct insights into future seasonal-scale changes in HAB risk for shellfish cultivation and harvesting, to inform optimal mitigation strategies (e.g., harvest scheduling).

### 2.2. Overview and Challenges of Existing Early Warning Systems

A number of real-time HAB monitoring systems have been coupled with short-term operational forecasting of HAB events in the coastal waters of Gulf of Mexico (Campbell et al., 2013; NOAA, 2021), Monterey Bay (Scholin et al., 2018), the Gulf of Maine (C. R. Anderson et al., 2019), the California coast (Kudela et al., 2021), and the Hong Kong coast (Yamahara et al., 2019). Short-term (3–5 days) and seasonal HAB forecasting systems are also operational in freshwater bodies, for example, Lake Erie, USA/Canada (National Centers for Coastal Ocean Science, 2024) and Lake Taihu, Jiangsu, China (Cao & Han, 2021). These various systems combine assessments of bloom location and extent (e.g., using remote satellite imaging and/or in situ monitoring data) with now casting and forecasting based on dispersion modeling and/or environmental predictors, such as seasonal variations in water temperature. Using this combined approach, an on-line HAB EWS has also been developed for shellfish farming areas in Scottish coastal waters (Davidson et al., 2021), where a “traffic light” index approach is used to highlight locations with elevated HAB/toxin risk, including *Dinophysis* spp. and OA toxins. This EWS was motivated by a number of human poisonings reported in 2013, following consumption of mussels harvested in the Scottish Shetland Islands (top-right of Figure 1). This event occurred during a time of exceptionally strong westerly winds that rapidly advected an offshore *Dinophysis* population to coastal shellfish aquaculture sites. The rate of increase in toxicity was greater than the 1-week resolution of the Official Control regulatory process and

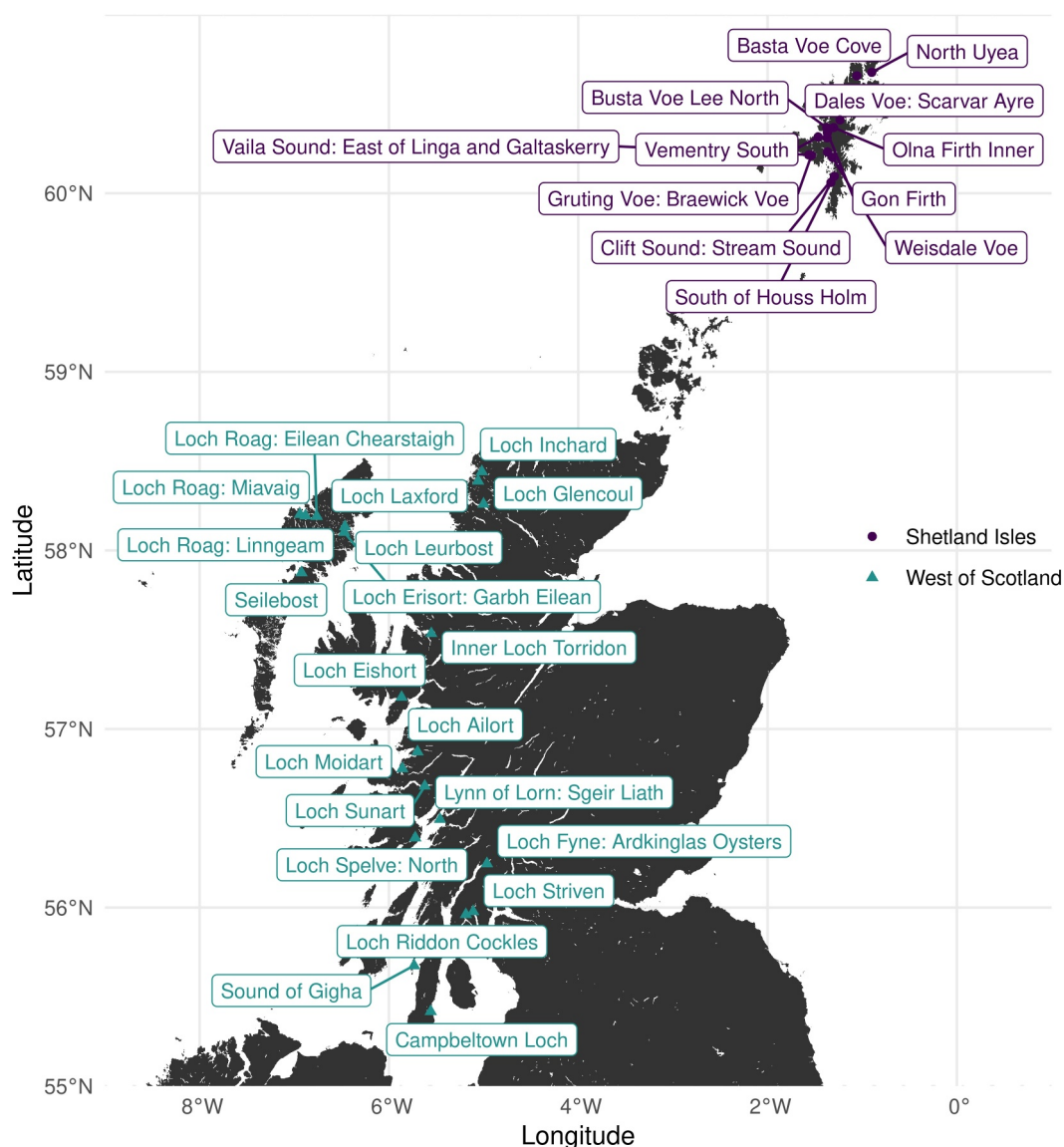


**Figure 1.** Locations of harvesting sites (circles and triangles) included in our predictive models, divided into two regions. Some site names are not labeled due to space constraints.

hence contaminated product reached consumers (Whyte et al., 2014). The EWS can enable tactical responses and mitigation of HAB risk through harvesting closure, but additional longer-term forecasting systems are required to inform more strategic measures, including spatial planning for new sites and mitigation of longer-term climate-driven impacts on shellfish aquaculture (Stoner et al., 2023).

Predicting HAB events is challenging due to multiple environmental drivers varying temporally from seconds to decades; and spatially from microscopic scales (mm) to mesoscales (100 km). These include physical factors driving water stratification, nutrient depletion, mixing, and nutrient replenishment, as well as ecological interactions between HAB species, other planktonic organisms, and their physico-chemical environment (D. M. Anderson et al., 2011; C. R. Anderson et al., 2019; Wells et al., 2020). Existing HAB models account for spatial and temporal variation in HAB risk either: explicitly in the case of dispersion models (Davidson et al., 2016) and mechanistic models incorporating key biogeochemical and ecological (life-history) processes (Gillibrand et al., 2016); or implicitly in the case of data models (i.e., statistical or machine learning models) that incorporate short-term and long-term trends (Davidson et al., 2016; Karasiewicz et al., 2020; Lima et al., 2022). Data models are simpler and less subject to structural errors, at the expense of overlooking physical processes. Moreover,

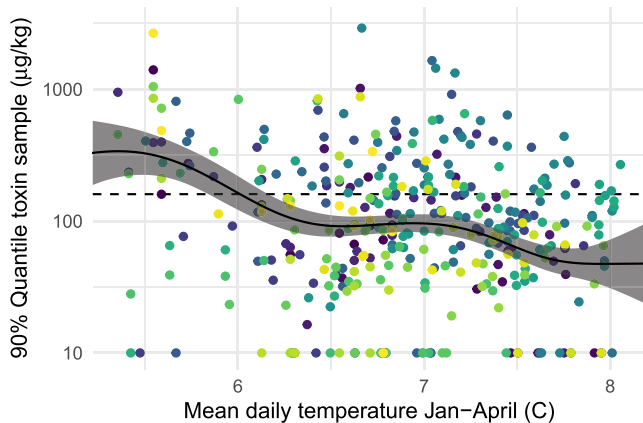


**Figure 2.** Mean winter-spring sea surface temperatures versus yearly toxin concentration “high points” (90% quantiles) in shellfish samples in Scotland, with colors representing different harvesting sites. The fitted line (with 95% confidence interval) shows the smooth function of mean winter-spring (first 120 calendar days) temperatures from the regression model described in Section 3.2. The horizontal dashed line shows the regulatory harvesting closure level (160  $\mu\text{g}/\text{kg}$  of shellfish flesh).

coupled with probabilistic elements, data models can quantify the uncertainty associated with any estimates or predictions (Lima et al., 2022).

Provided they are updated regularly (with new data), data models can be developed for generating short-term predictions of HAB events (Janssen et al., 2019), with the potential to inform short-term operational planning decisions for mariculture businesses (Wells et al., 2020). Recent approaches have demonstrated skill in making reliable short-term predictions, notably via flexible smoothing functions (Schmidt et al., 2018) or threshold functions accounting for sudden shifts, for example, when sea surface temperature falls below tolerable or optimal physiological limits for a HAB species (Taranu et al., 2017). Support vector machines, random forests, probabilistic graphical models, and artificial neural networks have also been shown to be capable of modeling highly dynamic (non-linear) and multi-source physico-chemical and biological data underlying HAB development and decay (Cruz et al., 2021; Grasso et al., 2019; Lee et al., 2003). These existing approaches, which mostly utilize meteorological and hydrographical variables as predictors, have tended to over-predict HAB duration (Davidson et al., 2016). While reassuring for human safety, this is not so appealing to businesses waiting for harvesting bans to be lifted (Brown et al., 2020).

Until now, accurate HAB forecasting using these various approaches has typically been limited to 1–2 weeks (Bedington et al., 2022; Cusack et al., 2016; Davidson et al., 2016, 2021; Schmidt et al., 2018). This short-term insight may be sufficient for preventing the harvesting of toxin contaminated shellfish but provides little warning for shellfish farmers to manage business risk and minimize the financial and reputational costs associated with sudden or late harvesting closures and shellfish poisoning. There is a clear need for new longer-term warning systems, so the aim of this work is to explore potential predictability of seasonal HAB severity and longevity based on preceding winter-spring sea surface temperature conditions.

### 2.3. Linking Winter-Spring Temperatures to HAB Impacts

Exploratory analysis of the Official Control data revealed a pattern of severe *Dinophysis* HAB events often following a colder-than-average winter-spring. Each point in Figure 2 represents 1 year and harvesting site in Scotland. The  $x$ -axis shows mean daily SSTs calculated over the first 120 days of each year (approximately January–April). The  $y$ -axis shows the 90<sup>th</sup> quantile of toxin concentration. The fitted regression curve (see Section 3.2 for details) reveals a very strong negative relationship; on average, a mean winter-spring SST of 8°C corresponds to a 90<sup>th</sup> quantile toxin concentration of 80  $\mu\text{g}/\text{kg}$ , while 5.5°C corresponds to 540  $\mu\text{g}/\text{kg}$ . Since the harvesting closure level is 160  $\mu\text{g}/\text{kg}$ , warmer or colder SSTs could mean the difference between a year with little disruption and a year with protracted closures. We do not claim to have demonstrated that the estimated SST-HAB association is causal, but argue that it may be useful for longer-term predictions than previously possible. We believe this is a novel insight for *Dinophysis* species, which is responsible for the vast majority of harvesting closures in Scotland.

### 2.4. Aims

Using the mean SST value as the predictive information behind an EWS is a considerable simplification of the potentially exploitable information offered by a complete time series of daily SSTs. We therefore require a flexible yet practical way of capturing all this information. We also require a framework that provides a more complete picture of the timing/longevity of predicted blooms and their impacts on aquaculture.

To meet these aims, we propose a regional EWS approach, driven by a flexible Generalized Additive Model framework that includes:

- Linear functional terms to capture the aggregate effect of temporally varying covariates (e.g., SST measured over 120 days of the year);
- Tensor product terms to allow for flexible structures, including spatial and temporal variation;

- Hierarchical structures to capture the features of individual harvesting sites more robustly, by pooling the data.

The framework can be adapted to either model the actual toxin concentrations or, as we present here, the probability of concentration exceeding a certain threshold. For the latter “classification” case, we use the threshold of 160  $\mu\text{g}/\text{kg}$  of OA equivalents, which is the regulatory closure level. In the following sections, we demonstrate how probabilistic predictions of future toxin values can be used to compute aggregate quantities that capture the severity and timing of regional HAB events. Prediction of such quantities could then form the essential input to an EWS.

### 3. Methodology

#### 3.1. Sea Surface Temperature Data

We downloaded SST data from the Copernicus Marine Service. For dates prior to 2021, we used hourly mean SST data from the Atlantic European North West Shelf Ocean Physics Reanalysis product (Copernicus Marine Service, 2024c), which has a spatial resolution of  $0.111^\circ \times 0.067^\circ$ , and computed daily mean values. For dates in 2021 and 2022, we used daily mean values from the European North West Shelf/Iberia Biscay Irish Seas High Resolution ODYSSEA L4 Sea Surface Temperature Analysis product (Copernicus Marine Service, 2024a), which has a spatial resolution of  $0.02^\circ \times 0.02^\circ$ . For each classified harvesting location in the Official Control data set, we matched both sets of SST data by finding the closest grid cell to the harvesting location with a complete time series of SST values (meaning no missing values, e.g., due to the grid cell being land instead of water). Distance between SST grid cells and classified harvesting locations was taken to be the Euclidean distance, calculated using longitude and latitude.

#### 3.2. Exploratory Analysis

Prior to developing the statistical early warning framework that constitutes the main body of this article, we carried out exploratory analysis to investigate a potential link between winter-spring SST to high *Dinophysis* toxin concentrations.

To achieve this, we pooled data across Scotland and carried out a univariate regression of 90<sup>th</sup> toxin quantiles against mean SST from the first 120 calendar days of the year (Figure 2). We fit a Generalized Additive Model (S. N. Wood, 2017) with a smooth function of mean SST and a random effect intercept for each site, assuming Gaussian errors for the log of the 90<sup>th</sup> quantiles. We have no physical rationale for the Gaussian assumption, so we checked it using a quantile-quantile plot of the deviance residuals, which indicated a good fit. The narrow width of the 95% confidence intervals in Figure 2 reflects the weight of evidence for the effect of SST. The model also significantly outperforms a reduced model without SST as a covariate ( $F$ -test with  $p$ -value =  $6.7 \times 10^{-13}$ ).

#### 3.3. General Framework

For a given year of interest, let  $y(t, s)$  denote toxin concentrations in a sample taken on day  $t$  at harvesting site  $s$ . Any statistical approach to modeling the whole range of possible values for  $y(t, s)$  would require assuming a flexible non-negative probability distribution, for example, log-Normal, or using a suitable transformation. In this paper, we focus on the impact of harvesting closures that occur when toxin concentrations in a shellfish sample exceed 160  $\mu\text{g}/\text{kg}$ . One option is therefore to construct and model the binary variable  $z(t, s) = \mathbb{I}(y(t, s) \geq 160 \mu\text{g}/\text{kg})$  as a Bernoulli quantity—as illustrated in Figure 3 for the Sandsound Voe shellfish harvesting site—and characterize the probability of a harvesting closure  $p(t, s) = P(z(t, s) = 1)$  with a logit-link or similar, viz:

$$z(t, s) \sim \text{Bernoulli}(p(t, s)); \quad (1)$$

$$\log\left(\frac{p(t, s)}{1 - p(t, s)}\right) = \eta(t, s). \quad (2)$$

This is a “logistic regression” model, one of most common ways of probabilistically modeling binary variables (Gelman et al., 2014; S. N. Wood, 2017). This approach is attractive here, first because modeling the exceedance

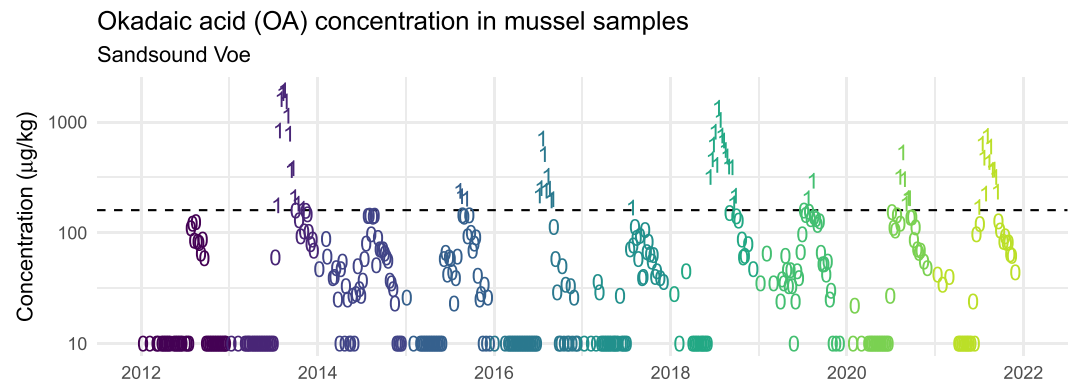


**Figure 3.** Okadaic acid concentrations in mussel samples, taken at Sandsound Voe, Shetland. The horizontal dashed line shows the regulatory harvesting closure level (160  $\mu\text{g}/\text{kg}$  per kilogram of shellfish flesh). Points are denoted 0 or 1 depending on whether or not the toxin level is greater than or equal to 160.

probability  $p(t, s)$  directly is more straightforward and second, because it requires no special treatment of “non-detect” toxin measurements. These records, which make up around 70% of the unfiltered data for Scotland, occur when the toxin concentration in a shellfish sample is too low for a reliable value to be recorded. Non-detects are prolific even for data-rich sites like Sandsound Voe: in Figure 3 non-detects are plotted as 10  $\mu\text{g}/\text{kg}$  for illustration. A rigorous modeling approach would need to either impute these values or, better still, treat them as left-censored (Kalbfleisch & Prentice, 2002). Conversely, because we can reasonably assume non-detects are below 160  $\mu\text{g}/\text{kg}$ , the corresponding values of  $z(t, s)$ , that is, the binary variable denoting whether a measurement is above or below the threshold 160  $\mu\text{g}/\text{kg}$ , can just be recorded as 0.

Next, we define four yearly statistics to capture the impact from HABs in a particular year: two that capture the overall severity of closures (closure proportion and (HAB) season duration) and two that capture the timing of closures (the day of first and final closure). More specifically:

- **Closure proportion:** Proportion of shellfish samples exceeding the harvesting closure threshold.
- **Season duration:** Time difference between the first and final closure.
- **First closure day:** Day on which the first sample exceeding the threshold is expected to be collected.
- **Final closure day:** Day on which the final sample exceeding the threshold is expected to be collected.

The statistics are initially computed for each harvesting site, but can then be aggregated to a regional-level: for example, the sample mean across sites. The closure proportion can be straightforwardly computed as  $n^{-1} \sum_{s,t} p(t, s)$  for the year of interest, where  $n$  is the number of samples in that year. The other three statistics can be computed using the following simulation procedure:

- Step 1: Simulate a large number  $j = 1, \dots, N$  (e.g.,  $N = 10000$ ) of new data sets of  $z^{(j)}(t, s)$  for the year of interest, using the estimated  $p(t, s)$ .
- Step 2: For each new data set  $j$ , define the first closure day  $t_{\text{first}}^{(j)}$  as the earliest  $t$  such that  $z^{(j)}(t, s) = 1$ , and the final closure day  $t_{\text{final}}^{(j)}$  as the latest  $t$  such that  $z^{(j)}(t, s) = 1$ . Compute the season duration as  $t_{\text{final}}^{(j)} - t_{\text{first}}^{(j)}$ . We thus have  $N$  samples for the three statistics of interest, forming a distribution that describes prediction uncertainty. The closure proportion can also be computed using this simulation procedure, if measures of uncertainty are desired.
- Step 3: For point estimates, compute the mean value of the samples for each statistic (for the first closure day, final closure day, and season duration, we exclude samples where there is not at least one  $z^{(j)}(t, s) = 1$  from this calculation).

We will focus on these four statistics as they are generally applicable, but using the above simulation approach there is scope to develop a wide range of alternative statistics, to best capture potential impacts in specific situations.

The main challenge is then constructing a model for  $\eta(t, s)$  that can flexibly capture complex covariate relationships and spatiotemporal heterogeneity—without over-fitting the relatively few years of data available—while at the same time ensuring “optimal” use of the data through pooling information via hierarchical

structures. In what follows, we explain how this can be achieved using Generalized Additive Models (GAMs) in the R package “mgcv” (S. N. Wood, 2011). The novelty of this work lies in the use of hierarchical GAMs combined with stochastic simulation, to develop an early warning framework where predictions/forecasts are explainable (e.g., to shellfish mariculture industry or regulatory bodies) based on estimated effects of preceding oceanographical conditions. Details on standard GAM methodology and functionality are given in Text S1 in Supporting Information S1. Then, in Section 4, we apply a single model formulation to Official Control data from two regions in Scotland.

### 3.4. Linear Functional Terms

Central to the problem of defining a suitable model for generating early warnings is the need to capture effects from covariates that are temporally varying, for example, winter-spring SST. Let  $SST_{d,s}$  be the mean daily SST measured on day  $d \leq D$  of the year of interest (i.e., where  $d = 1$  is the 1st of January), at harvesting location  $s$ . Note that we now have two different time indices:  $t$  are the days of the year the shellfish samples are collected on and  $d$  are the days the SST values are measured on. Then, suppose we wish to estimate the relationship between the first 4 months of SST values ( $D = 120$ ) and the probability  $p(t, s)$  of a future shellfish sample having a toxin concentration above the harvesting closure threshold (160  $\mu\text{g}/\text{kg}$ ). That is, we will have SST data for days  $d = 1, \dots, 120$  and will model/predict  $p(t, s)$  from day  $t = 121$ , up to a maximum of 365 (or 366 in a leap year). We could model  $p(t, s)$  using a linear predictor (Equation 2) composed of all  $D = 120$  SST values as:

$$\eta(t, s) = \beta_0 + \sum_{d=1}^D \beta_d SST_{d,s}. \quad (3)$$

The first problem with this approach is that there is likely to be strong correlation/collinearity between consecutive SST measurements, inflating the standard errors for estimated  $\beta_d$ . A further issue is that the large number of coefficients (e.g., 120  $\beta_d$ 's) might lead to over-fitting, resulting in poor out-of-sample performance and increased uncertainty.

One way to deal with these issues, is to a priori constrain the values of the coefficients in (Equation 3) so that they are not independent. This can be achieved by assuming the coefficients are the output of a smooth function of  $d$  that is,

$$\beta_d = f(d). \quad (4)$$

This is straightforward to implement using the mgcv package, which also allows for non-linearity in the effect of SST via

$$\eta(t, s) = \beta_0 + \sum_{d=1}^D f(SST_{d,s}, d), \quad (5)$$

where  $f()$  is now a 2-D smooth function. More generally, tensor product smooths (Text S1.2 in Supporting Information S1) can be used to capture the aggregated effects of one or more covariates, as a function of  $d$ , in a non-linear way. As an illustrative example, (Equation 5) could be extended to

$$\eta(t, s) = \beta_0 + \sum_{d=1}^D f(RAIN_{d,s}, SST_{d,s}, d), \quad (6)$$

where in this case the function  $f()$  captures the non-linear effect of SST as a non-linear function of daily precipitation ( $RAIN_{d,s}$ ), also measured on days  $d \leq D$ . Furthermore, we can add multiple linear functional terms additively.

### 3.5. Hierarchical Structures

Within the GAM framework, we can also construct hierarchical spline structures that optimize the use of the data by pooling information, and that aid interpretation of the model by identifying patterns (trends) that are common across various groups in the data. There are various ways of achieving this using GAMs (Pedersen et al., 2019), but here we opt for a way that maximizes flexibility while at the same time achieves some data pooling. Specifically, we utilize a hierarchical structure to identify a common seasonal trend across sites, while allowing each site to have its own seasonal cycle—as a deviation from the common one. Recall that  $t$  is the day of the year on which a shellfish sample is collected and that we are modeling/predicting threshold breach probabilities  $p(t, s)$  for future days relative to the SST data ( $t > D$ ), then

$$g(t) + h_s(t); \quad t > D \quad (7)$$

defines an overall (mean) seasonal cycle  $g(t)$  across all sites plus the site-specific “deviation”  $h_s(t)$ . The splines  $h_s(t)$  are constrained to be centered on  $g(t)$ , so information pooling is achieved through  $g(t)$ , while individual site seasonal behavior is captured by  $g(t) + h_s(t)$ . To better identify between  $g(\cdot)$  and  $h_s(\cdot)$ , the penalty of the site-specific terms  $h_s(\cdot)$  is on the first derivative of  $h_s(\cdot)$  instead of the second derivative, which is the case for  $g(\cdot)$  (Pedersen et al., 2019). This also means that the deviations  $h_s(\cdot)$  can be individually “shrunk” to zero if the evidence is weak.

### 3.6. Model Formulation

In carrying out this work we developed a range of alternative model configurations, including extensions to account for structured spatial variability, and compared prediction performance for these when applied to the Shetland Islands and to the West of Scotland, using the out-of-sample experimental approach described later in Section 3.7. The full list of alternative formulations and the results from the comparison are given in: Text S2 and S3 in Supporting Information S1. Here, we present the formulation for what we believe is the most elegant model, which had the best performance across both study regions.

Recall that  $\eta(t, s)$  is our predictor function for the probability of a shellfish sample taken on day  $t$  and at site  $s$  having a toxin concentration exceeding 160  $\mu\text{g}/\text{kg}$ . The model is then characterized by:

$$\eta_{t,s} = \alpha + \delta_s + \epsilon_{year,s} + \sum_{d=1}^D [f(SST_{d,s}, d)] + g(t) + h_s(t). \quad (8)$$

The first term on the right hand side of Equation 8 is an intercept term  $\alpha$ , that captures the average probability of exceedance over time and across sites, when all covariates are at their mean (i.e., when all other terms are equal to zero). Next,  $\delta_s$  is an independent, identically distributed (i.i.d.) Gaussian random effect term (see: Text S1.1 in Supporting Information S1) that captures site-specific deviations from  $\alpha$  in the overall probability of an exceedance:

$$\delta_s \sim \text{Normal}(0, \sigma_\delta^2). \quad (9)$$

The advantage of assuming a random effect, rather than a fixed effect, is that estimation of  $\delta_s$  is more stable and less uncertain for sites with little or no data. The latter scenario may occur, for example, when a new harvesting location opens. The next term,  $\epsilon_{year,s}$ , is an i.i.d. Gaussian random effect for each year and site combination:

$$\epsilon_{year,s} \sim \text{Normal}(0, \sigma_\epsilon^2), \quad (10)$$

whose purpose is to explicitly capture annual variability in the severity of HAB events at each site. Without this term, the model can only describe systematic annual variability through the covariate effects, which could plausibly result in over-fitting. With  $\epsilon_{year,s}$ , the model can optimally trade-off structured variability through the covariate effects and unstructured variability through the random effect. In the development of this model and



those tested in Supporting Information S1, we found that including  $e_{year,s}$  significantly reduced out-of-sample prediction errors for unseen years.

Next,  $f(SST_{d,s}, d)$  is the linear functional term for SST, in this case a 2-D tensor product of SST and SST measurement day  $d$ . The SST and  $d$  tensor product is composed of thin-plate spline marginal bases with 5 knots each, meaning the maximum degrees of freedom of  $f(SST_{d,s}, d)$  is  $5^2 - 1 = 24$ . Note that choosing the number of knots for each smooth term is standard practice for fitting GAMs, and generally amounts to a trade-off between computation time and the upper limit on flexibility (S. N. Wood, 2017). Our choices here reflect what was computationally practical in the context of the out-of-sample prediction experiment detailed in Section 3.7 and in the context of comparing multiple alternative model formulations of varying complexity (Text S2 and S3 in Supporting Information S1). Further study may be needed to determine the optimal number of knots for a given application of the model.

We then add seasonal structure over the prediction time period through the combined effect of two terms. The first,  $g(t)$ , is a 1-D thin-plate spline with 10 knots. It therefore captures the average seasonal cycle in *Dinophysis* toxin levels across all harvesting sites in the region. Then,  $h_s(t)$  captures site-specific deviations from  $g(t)$ . Each  $h_s(t)$  has a first-order smoothness penalty, meaning they can be shrunk to zero for sites where there is weak evidence of an unusual seasonal cycle (Section 3.5). Conceptually,  $g(t)$ , and  $h_s(t)$  define the expected shape of an annual bloom cycle at site  $s$ , and through  $f(SST_{d,s}, d)$ , the SST can shift this shape down or up to predict blooms that are shorter in duration or are more persistent.

### 3.7. Yearly Prediction Experiment

To investigate the potential strengths and weaknesses of our proposed early warning models, we performed out-of-sample prediction experiments. The experiments aim to imitate operational use of these models for generating yearly regional HAB warnings. For each year in 2012–2021 inclusive, we followed the below procedure:

- Step 1: Withhold all data for that year.
- Step 2: Fit all the models to be tested to the data for the remaining years.
- Step 3: Generate predictions of the four statistics described in Section 3 for the out-of-sample year, using each of the models.
- Step 4: Compute regional aggregates of the four statistics, by computing their sample mean across all sites.

We note two ways in which the procedure might not be perfectly realistic. The first is that training data can include future years relative to the out-of-sample year. We made this decision to maintain a relatively consistent quantity of training data for each out-of-sample year. However, we believe it does not affect the validity of results as all the models we present assume years are exchangeable (i.e., we do not assume any between-year temporal structure).

Second, the simulation procedure for the HAB statistics described in Section 3 relies on specifying shellfish sample collection dates. It should be noted that some of the yearly variability in the four statistics can likely be attributed to the distribution of these dates. For instance, if samples are mainly collected during the winter in 1 year, then we would expect the closure proportion to be lower due to *Dinophysis* being less abundant during the winter. The compromise in realism here is that we use the known collection dates when predicting unseen years. To limit the impact of irregular sampling schedules on the variability of the four statistics, we filter the data to year-site combinations with at least 30 shellfish samples. Though arbitrary, we chose this cut-off as we believe 30 or more samples in a given site and year has good potential to capture a HAB event evenly. We discuss how one might account for unknown sample dates in Section 5.

### 3.8. Baseline Same Mean Prediction Approach

We compare prediction performance for the model presented in Section 3.6, and the models presented in Supporting Information S1, against a baseline (null) “sample mean” model. This baseline model involves predicting the four statistics in an out-of-sample year as their sample mean across all in-sample years. This procedure replaces Steps 1–3 above, while Step 4 is still needed to compute regional aggregates.

## 4. Results

### 4.1. Application to the Shetland Isles and West of Scotland

Shetland, or the Shetland Isles, is an archipelago about 170 km north-east of the Scottish mainland. Aquaculture has always been an important part of the local economy, and mussel harvesting in Shetland has reached about 80% of the total Scottish production (Promote Shetland, 2022). In the 10 year period 2012–2021, Shetland faced 5 non-consecutive years of relatively low disruption from *Dinophysis* HABs (where 0.3%–1.9% of samples were above 160  $\mu\text{g}/\text{kg}$  OA equivalents in total across all sites) and 5 years with relatively high disruption (where 7.6%–30.6% of samples were above 160  $\mu\text{g}/\text{kg}$ ). An EWS driven by a predictive model that accurately forecasts severe HAB seasons could therefore aid the Shetland shellfish industry in planning for disruption. Here, the maximum distance between any two sites is 90 km, indicating a high density of data over a relatively small spatial extent (with respect to large-scale climatological and oceanographic variation).

Shellfish industry is well established throughout the western coast of Scotland and the Western Isles, with production taking place in coastal and inland sea lochs, as well as more open and exposed coastal sites employing bottom (bed) cultivation and suspended aquaculture methods. Here, the maximum distance between sites is 345 km, meaning a similar quantity of data as for Shetland is spread more thinly over a much larger geographical extent. At the same time, we might expect more substantial spatial variation in HAB seasonal cycles and covariate relationships, due to heterogeneous climatological and ocean regimes in different parts of the region (e.g., in the far-north vs. the far-south).

For the application of our framework, we chose to focus on harvesting sites with an established history of monitoring shellfish samples and with non-trivial toxin levels. Between 2009 and 2022, harvesting sites had a mean of 48.5 samples with detectable toxin levels (in the unfiltered data set). We chose to reduce the data to (a) sites with at least 50 of these samples and (b) year-site combinations with at least 30 samples (including non-detects), to reduce the impacts of irregular scheduling (see Section 3.7).

For the Shetland Isles, these criteria result in 3,579 samples after calendar day 120 (Table 1), across 14 unique classified harvesting sites—all of these samples were common mussels. Of these samples, 382 (11%) had OA toxin levels above the closure threshold of 160  $\mu\text{g}/\text{kg}$ . For the West of Scotland, the filtering criteria result in 3,361 shellfish samples after calendar day 120, across 21 distinct classified harvesting areas. About 95% of these samples (3,180) were common mussels, a further 176 were pacific oysters, 4 were common cockles, and 1 was razors. Of these, 532 (16%) had OA toxin levels at or above the harvesting closure threshold (160  $\mu\text{g}/\text{kg}$ ).

### 4.2. Interpreting Model Outputs

We first show how the estimated functions can be visualized and interpreted, to better understand and communicate what drives predictions and gain insights into what situations may indicate the most severe HAB risks. Here we explore visualizations for the Shetland Islands, as an illustrative example. Figure 4 shows the estimated effect of daily SST values on the probability of a mussel sample exceeding 160  $\mu\text{g}/\text{kg}$  OA equivalents. “Trajectories” of actual SST values from Sandsound Voe are shown for different years using symbols. Brighter green-yellow areas multiplicatively increase the probability of exceedance  $p(t, s)$  if SST passes through them, whereas darker blue-purple areas reduce the probability. The plot suggests that spring SSTs (i.e., March to late April) have the greatest impact, with colder temperatures being associated with higher summer toxin levels.

In Figure 3, we can see that the two most severe blooms occurred in 2013 and 2018, with weaker blooms occurring in adjacent years. Looking at the actual SSTs for those years in Figure 4, we can see a clear distinction between the two most severe years (2013 and 2018)—which had much colder SST values—and the adjacent years.

Figure 5 shows estimated seasonal cycles for the probability of shellfish samples exceeding harvesting closure levels for OA toxicity. The black line shows the estimated average cycle ( $g(t)$ ) for the Shetland Isles, suggesting the probability of exceedance is highest in August. The relationship is very strong, as evidenced by the narrowness of the 95% confidence intervals (shaded area). The colored dashed lines are the site-specific seasonal cycles: the sum of  $g(t)$  and  $h_s(t)$ . Many sites have seasonal cycles close to or almost equal to the overall average cycle  $g(t)$ , which occurs when there is insufficient evidence that a given site has a distinct seasonal cycle. As such, the

**Table 1**  
*Counts of Shellfish Samples After Calendar Day 120 at Each Harvesting Site, After Applying Site Selection Criteria (Section 4.1), Where “No.” Means “Number”*

Harvesting site	No. of samples	No. of non-detects	No. exceeding 160 µg/kg OA eq.
<b>Shetland</b>			
Aith Voe Sletta	288	132	27
Basta Voe Cove	317	235	14
Busta Voe Lee North	289	142	23
Clift Sound: Stream Sound	284	130	36
Dales Voe: Scarvar Ayre	311	148	38
Gon Firth	188	85	14
Gruting Voe: Braewick Voe	307	118	37
North Uyea	40	7	8
Olna Firth Inner	280	166	23
Sandsound Voe	309	97	60
South of Houss Holm	113	62	17
Vaila Sound: East of Linga	321	151	21
Vementry South	281	152	22
Weisdale Voe	251	80	42
<b>West of Scotland</b>			
Campbeltown Loch	254	46	42
Inner Loch Torridon	179	24	66
Loch Ailort	63	11	6
Loch Eishort	311	73	96
Loch Erisort: Garbh Eilean	112	53	2
Loch Fyne: Ardkinglas Oysters	175	126	12
Loch Glencoul	112	55	22
Loch Inchard	89	30	28
Loch Laxford	180	51	60
Loch Leurbost	190	120	6
Loch Moidart	88	45	16
Loch Riddon Cockles	159	42	11
Loch Roag: Eilean Chearstaigh	237	112	23
Loch Roag: Linngeam	280	117	34
Loch Roag: Miavaig	247	108	26
Loch Spelve: North	64	43	0
Loch Striven	102	7	72
Loch Sunart	60	27	5
Lynn of Lorn: Sgeir Liath	167	130	0
Seilebost	166	111	4
Sound of Gigha	126	71	1

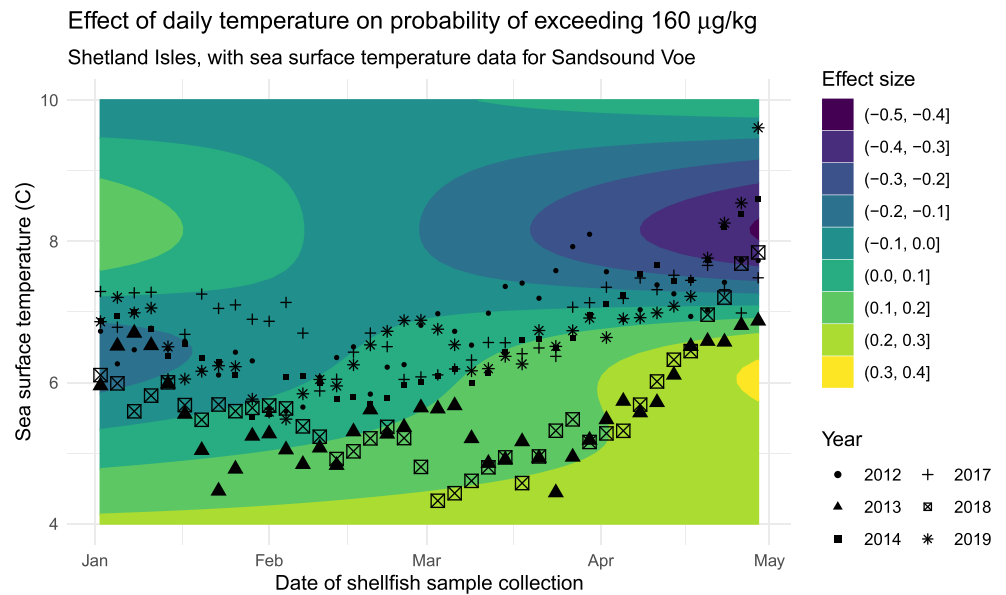


**Figure 4.** Colored surface: estimated effect of daily SST (y-axis) for each of the first 120 days of the year (x-axis) on the probability (logit scale) of a sample being over 160 µg/kg okadaic acid equivalents. Symbols: daily temperature values (plotted at 3-day intervals) for different years in Sandsound Voe, Shetland. The size of the shapes is proportional to the number of closures in that year.

penalized hierarchical structure has resulted in a more constrained model here, compared to one with independent site-specific seasonal cycles.

### 4.3. Predictive Performance

Next, we discuss out-of-sample prediction performance for the four HAB statistics, from the yearly prediction experiment (Section 3.7). Figure 6 shows out-of-sample predictions (x-axis) versus values computed from the observed data (y-axis) for each of the four statistics (columns), by region (rows). For the two statistics relating to overall HAB severity, closure proportion and season duration, there is a strong correspondence between the out-of-sample predictions and the observed values. The predictions appear to be consistently good, from the years with the fewest closures and the shortest durations, up to the years with the most closures and the longest durations. Mean Absolute Error (MAE) values (MAE) for these two statistics (Table 2) were substantially lower

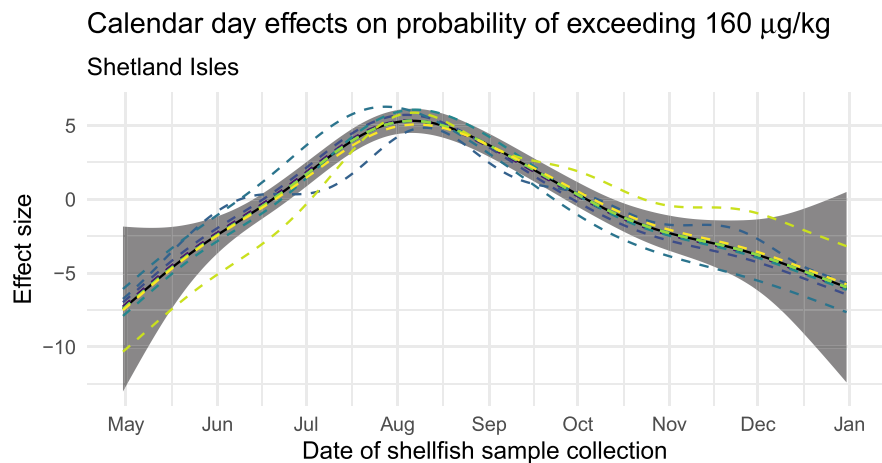


**Figure 5.** Estimated Shetland Isles main effect  $g(t)$  of the day of sample collection ( $t$ ) on the probability of the sample exceeding 160 µg/kg of shellfish flesh okadaic acid equivalents (solid black line), with 95% confidence interval (shaded area), and site-specific calendar day effects  $g(t) + h_s(t)$  (colored dashed lines for each site).

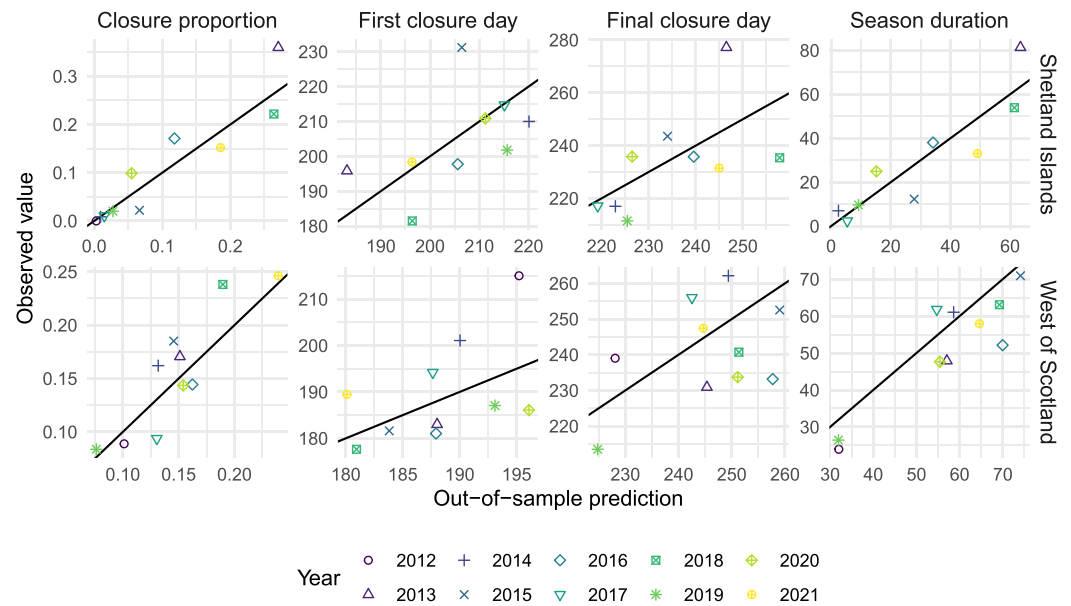


**Figure 6.** Yearly out-of-sample predictions for each of the four Harmful Algal Bloom statistics (closure proportion, season duration (days), first closure day, final closure day) for the Shetland Islands (top row) and the West of Scotland (bottom row). The black lines are diagonal  $y = x$  lines.

when predicting from the model versus the baseline sample mean approach (Section 3.8). Gains over the baseline were greatest, in relative terms, for Shetland.

For the two statistics that quantify the timing of HAB events, first closure day and final closure day, Figure 6 shows some correspondence between the out-of-sample predictions and the observed values. For data from Shetland, the model predictions offered sizable reductions in the MAEs for these two statistics (Table 2), compared to the baseline. For the West of Scotland, the model offered a modest reduction in MAE for the first closure day, but this is offset by the model having a higher MAE for the final closure day.

### 5. Discussion

Motivated by a need for longer-term predictions of future HAB impacts, we developed a flexible conceptual framework combining multiple advanced structures that can be fitted using the Generalized Additive Model (GAM) engine. Most notably, we demonstrated how linear functional terms can capture the effect of temporally varying covariates, notably SST, on phycotoxin levels in shellfish. While these terms can be as complex as needed, for example, to capture spatial variation, they can be fully visualized and interpreted to potentially advance understanding of the environmental drivers of severe HAB events.

Combining Official Control data on weekly phycotoxin concentrations (i.e., *Dinophysis* toxin concentrations in OA equivalents) in cultivated shellfish and satellite observation data quantifying daily sea surface temperatures

**Table 2**  
Mean Absolute Error When Predicting the Four Regionally-Aggregated Harmful Algal Bloom Statistics in the Yearly Prediction Experiments

Region	Prediction Method	Closure proportion	First closure day	Final closure day	Season duration
Shetland	Baseline	0.11	13	18	27
	<b>Model</b>	<b>0.03</b>	<b>9.5</b>	<b>12</b>	<b>8.2</b>
West of Scotland	Baseline	0.055	10	11	9.3
	<b>Model</b>	<b>0.024</b>	<b>7.7</b>	<b>13</b>	<b>7.2</b>

Note. The “Baseline” rows refer to the baseline sample mean prediction approach detailed in Section 3.8, while “Model” (highlighted in bold) refers to our proposed model detailed in Section 3.6

around Scotland, we have presented compelling evidence for a predictive link between winter-spring SSTs and summer OA levels in shellfish samples. In both the regions studied (Western Scotland and the Shetland Isles), colder winter-spring sea surface temperatures were associated with higher *Dinophysis* toxin levels in shellfish sampled in the following summer. Below, we outline the ecological life-history processes of encystment, quiescence and germination in dinoflagellates, which could potentially underpin this association.

Declining water temperatures during the winter-spring prompt dinoflagellates (including *Dinophysis spp.*) to form dormant cysts, which can survive extended periods of unfavorable environmental conditions (D. M. Anderson et al., 2014). Increasing temperatures in the spring provide a cue for cysts to enter a quiescent state, in which they will germinate if other environmental conditions (e.g., light, nutrient and predator/prey levels) become favorable (Pfiester & Anderson, 1987). Recent work on the dinoflagellate *Alexandrium catenella* has shown that germination of quiescent cysts is primed by chilling, that is, cumulative exposure to cold temperatures below a threshold, which prevents precocious germination during short spells of favorable conditions in otherwise unfavorable seasons (Fischer et al., 2018). We hypothesize that chilling during an especially cold winter/spring provides a strong signal for synchronising the germination of *Dinophysis* cyst beds in our study region (including cysts which may have been dormant for several years), thus forming a substantial pulse of germinating cells with rising temperatures in the following spring/summer. This hypothesis is consistent with evidence that chilling shortens dormancy and improves the viability of cysts from other dinoflagellates, including *Alexandrium pseudogonyaulax* (Montresor & Marino, 1996), *Gymnodinium pseudopalustre* and *Woloszynskia apiculata* (von Stosch, 1973).

We carried out a yearly prediction experiment that aimed to imitate real-world operational use of the models we presented, as realistically as possible. With all retrospective experiments it is challenging to achieve perfect realism and here we have sought to transparently explain two ways in which we feel this is not achieved. Notably, we explained the issue of needing to know the scheduled shellfish sampling dates to make predictions of the four HAB statistics. If we did not know the collection dates, we could randomly simulate sampling dates during the simulation of the statistics, to capture the additional uncertainty associated with unknown collection dates. This simulation could be based on re-sampling previous years or on a second logistic regression model for the probability of a sample being collected or not on a given date. However, it should be noted that this imperfection is largely related to the specific statistics we defined. Alternative statistics that capture the impact of HABs—for example, the proportion of samples above 160  $\mu\text{g}/\text{kg}$  OA equivalents if a sample were hypothetically collected every day—would not necessarily suffer from this problem.

Nonetheless, we believe predicting whole unseen years of data is a very unforgiving experimental design and that the improvements in accuracy presented here are notable. For the Shetland Islands, the average errors for the closure proportion and the season duration were cut down by about 70%, compared to the baseline sample mean approach. Modest but noteworthy reductions of about 30% in the mean absolute errors were achieved when predicting the first and last closure days.

When comparing a wider cohort of non-spatially structured models (Text S2 in Supporting Information S1), we found the model presented in the main article is an apparent “sweet-spot” in complexity, performing well overall while more complex models actually demonstrated increased mean absolute errors. With the more complex models, we explored higher-dimensional interactions between SST and shellfish collection date, which aimed to capture the relationship between SST conditions and the timing of HAB events better. With more data, it may be possible to estimate these terms without worse out-of-sample prediction performance from over-fitting.

The same model design performed strongly when predicting unseen years in the West of Scotland. Once again, the MAE for the closure proportion was significantly reduced compared to the baseline sample mean approach, in this case by about 60%. In Text S3 in Supporting Information S1, we tested extensions of this model that included smooth spatial structures, which did not improve prediction accuracy at a regional level. The reason for this may be that the spatial variation in the data is inherently non-smooth, due to coastal boundaries or local geographies. The lack of improvement from including smooth spatial structures could also indicate that the hierarchical term  $h_s(\text{day})$  is effective at making the model robust to variation between sites in HAB seasonality.

Overall, we believe it is extremely promising that a single model design was able to perform well in two regions independently. Larger reductions in modeling error were achieved in the Shetland Isles, which represents the best case scenario between the two regions as Shetland had a high density of shellfish toxin data over a relatively small

area. As things stand, we believe this model could plausibly be refined into an annual warning system for HABs in Scotland by regulators or industry. We relied on only the first 120 days of sea surface temperature measurements each year, allowing for predictions of the summer HAB season to be generated in early May.

This improved insight into the severity of seasonal *Dinophysis* toxin concentrations, which could be made available annually in April/May (the typical onset of the *Dinophysis* bloom season), would be highly advantageous to aquaculture businesses and regulators. Practical benefits could include; informing harvest scheduling; directing harvesting activities to alternative shellfish sites; enabling better resource (including human resource) planning and supply chain management. Further advantages from predicting the likely onset of blooms include better targeting and intensification of end-product testing (including in situ testing) to better protect shellfish businesses and consumers.

Further research could explore predictions made earlier or later in the year, and quantify impacts on prediction performance. Notably, in our experiments we treated whole years of data as unseen. In real-world operational use, models fitted within our conceptual framework could be updated as the year progresses and as more Official Control data becomes available, and used to generate site-specific shorter-term forecasts. Our framework can be adapted for this purpose by simply replacing the fixed time window in the linear functional terms (here, the first 120 days in the year) with lagged covariate inputs relative to the prediction date (e.g., the previous 120 days), as in Brown et al. (2022). While we focused on the impact of winter-spring SST on HABs here, the integrative effect of other temporally-varying covariates, such as insolation, salinity, nutrient levels, wave height, wave speed and direction could also be included using new linear functional terms or even interacted with SST using higher-dimensional tensor product smooths. This has the potential to reveal new insights into the drivers of HAB impacts and deliver more accurate predictions beyond the already promising results seen here.

### Conflict of Interest

The authors declare no conflicts of interest relevant to this study.

### Data Availability Statement

The biotoxin data and sea surface temperature used in the study for statistical modelling are available at Zenodo (Stoner et al., 2022). Conditions for use of the sea surface temperature data are detailed in the Copernicus Marine Service License (Copernicus Marine Service, 2024b).

Version 1.0.0 of the R code used to produce all results in this article is preserved at Zenodo (Stoner et al., 2022), available subject to a Creative Commons Attribution 4.0 International license.

### Acknowledgments

O. Stoner and A. R. Brown were funded by UK Department for Business, Energy & Industrial Strategy Regulators' Pioneer Fund and A. R. Brown was funded by the European Maritime and Fisheries Fund (ENG3103). T. Economou was funded by the European Union's Horizon 2020 research and innovation programme, under grant agreement No. 856612, and by the Cyprus Government. This study has been conducted using E.U. Copernicus Marine Service Information; <https://doi.org/10.48670/moi-00059>; <https://doi.org/10.48670/moi-00152>.

### References

- Anderson, C. R., Berdalet, E., Kudela, R. M., Cusack, C. K., Silke, J., O'Rourke, E., et al. (2019). Scaling up from regional case studies to a global harmful algal bloom observing system. *Frontiers in Marine Science*, 6(250). <https://doi.org/10.3389/fmars.2019.00250>
- Anderson, D. M., Cembella, A. D., & Hallegraeff, G. M. (2011). Progress in understanding harmful algal blooms: Paradigm shifts and new technologies for research, monitoring, and management. *Annual Review of Marine Science*, 4(1), 143–176. <https://doi.org/10.1146/annurev-marine-120308-081121>
- Anderson, D. M., Keafer, B. A., Kleindinst, J. L., McGillicuddy, D. J., Martin, J. L., Norton, K., et al. (2014). Alexandrium fundyense cysts in the gulf of Maine: Long-term time series of abundance and distribution, and linkages to past and future blooms. *Deep Sea Research Part II: Topical Studies in Oceanography*, 103, 6–26. <https://doi.org/10.1016/j.dsr2.2013.10.002>
- Bedington, M., García-García, L. M., Sourisseau, M., & Ruiz-Villarreal, M. (2022). Assessing the performance and application of operational Lagrangian transport HAB forecasting systems. *Frontiers in Marine Science*, 9. <https://doi.org/10.3389/fmars.2022.749071>
- Belin, C., Soudant, D., & Amzil, Z. (2021). Three decades of data on phytoplankton and phycotoxins on the French coast: Lessons from rephy and rephytox. *Harmful Algae*, 102, 101733. <https://doi.org/10.1016/j.hal.2019.101733>
- Berdalet, E., Fleming, L. E., Gowen, R., Davidson, K., Hess, P., Backer, L. C., et al. (2016). Marine harmful algal blooms, human health and wellbeing: Challenges and opportunities in the 21st century. *Journal of the Marine Biological Association of the United Kingdom*, 96(1), 61–91. <https://doi.org/10.1017/S0025315415001733>
- Bresnan, E. (2003). Monitoring programme for toxic phytoplankton in Scottish waters: 1st April 2002 - 31st march 2003 (Tech. Rep. No. 14/03). *Fisheries Research Services*, 45, 692–703. Retrieved from <http://www.frs-scotland.gov.uk/FRS.Web/Uploads/Documents/1403.pdf>
- Bresnan, E., Arévalo, F., Belin, C., Branco, M. A., Cembella, A. D., Clarke, D., et al. (2021). Diversity and regional distribution of harmful algal events along the Atlantic margin of Europe. *Harmful Algae*, 102, 101976. <https://doi.org/10.1016/j.hal.2021.101976>
- Brown, A. R., Lilley, M., Shutler, J., Lowe, C., Artioli, Y., Torres, R., et al. (2020). Assessing risks and mitigating impacts of harmful algal blooms on mariculture and marine fisheries. *Reviews in Aquaculture*, 12(3), 1663–1688. <https://doi.org/10.1111/raq.12403>
- Brown, A. R., Stoner, O., Kay, S., Turner, A., McQuillan, J., & Bage, T. (2022). Artificial intelligence approaches for predicting harmful algal blooms (HABs). (BEIS Regulators Pioneer Fund Report No. RPF Report v.1). UK Department for Business, Energy and Industrial Strategy. Retrieved from <http://hdl.handle.net/10871/131733>

- Campbell, L., Henrichs, D. W., Olson, R. J., & Sosik, H. M. (2013). Continuous automated imaging-in-flow cytometry for detection and early warning of karenia brevis blooms in the gulf of Mexico. *Environmental Science and Pollution Research International*, 20(10), 6896–6902. <https://doi.org/10.1007/s11356-012-1437-4>
- Cao, H., & Han, L. (2021). Hourly remote sensing monitoring of harmful algal blooms (HABs) in Taihu lake based on goci images. *Environmental Science and Pollution Research*, 28(27), 35958–35970. <https://doi.org/10.1007/s11356-021-13318-6>
- Copernicus Marine Service. (2024a). European north west shelf/Iberia Biscay Irish seas – High resolution odyssey I4 sea surface temperature analysis. E.U. Copernicus Marine Service Information (CMEMS) [Dataset]. *Marine Data Store (MDS)*. <https://doi.org/10.48670/moi-00152>
- Copernicus Marine Service. (2024b). Service commitments and licence [Licence agreement]. Retrieved from <https://marine.copernicus.eu/user-corner/service-commitments-and-licence>
- Copernicus Marine Service. (2024c). Atlantic-European north west shelf-ocean physics reanalysis. E.U. Copernicus Marine Service Information (CMEMS) [Dataset]. *Marine Data Store (MDS)*. <https://doi.org/10.48670/moi-00059>
- Cruz, R. C., Reis Costa, P., Vinga, S., Krippahl, L., & Lopes, M. B. (2021). A review of recent machine learning advances for forecasting harmful algal blooms and shellfish contamination. *Journal of Marine Science and Engineering*, 9(3), 283. <https://doi.org/10.3390/jmse9030283>
- Cusack, C., Dabrowski, T., Lyons, K., Berry, A., Westbrook, G., Salas, R., et al. (2016). Harmful algal bloom forecast system for SW Ireland. part II: Are operational oceanographic models useful in a HAB warning system. *Harmful Algae*, 53, 86–101. <https://doi.org/10.1016/j.hal.2015.11.013>
- Davidson, K., Anderson, D. M., Mateus, M., Reguera, B., Silke, J., Sourisseau, M., & Maguire, J. (2016). Forecasting the risk of harmful algal blooms. *Harmful Algae*, 53, 1–7. <https://doi.org/10.1016/j.hal.2015.11.005>
- Davidson, K., Whyte, C., Aleynik, D., Dale, A., Gontarek, S., Kurekin, A. A., et al. (2021). Habreports: Online early warning of harmful algal and biotoxin risk for the Scottish shellfish and finfish aquaculture industries. *Frontiers in Marine Science*, 8(350). <https://doi.org/10.3389/fmars.2021.631732>
- European Commission. (2004a). Regulation (ec) no 852/2004 of the European parliament and of the council of 25 June 2004 on the hygiene of foodstuffs [Government Document]. Retrieved from <https://eurlex.europa.eu/LexUriServ/LexUriServ.do?uri=OJ:L:2004:226:0003:0021:EN:PDF>
- European Commission. (2004b). Regulation (EC) no 853/2004 of the European parliament and of the council of 29 April 2004 laying down specific hygiene rules for food of animal origin [Government Document]. Retrieved from <https://eur-lex.europa.eu/LexUriServ/LexUriServ.do?uri=OJ:L:2004:139:0055:0205:en:PDF>
- European Commission. (2004c). Regulation (EC) no 854/2004 of the European parliament and of the council of 29 April 2004 laying down specific rules for the organisation of official controls on products of animal origin intended for human consumption [Government Document]. Retrieved from <https://eur-lex.europa.eu/LexUriServ/LexUriServ.do?uri=OJ:L:2004:226:0083:0127:EN:PDF>
- Fischer, A. D., Brosnahan, M. L., & Anderson, D. M. (2018). Quantitative response of Alexandrium Catenella cyst dormancy to cold exposure. *Protist*, 169(5), 645–661. <https://doi.org/10.1016/j.protis.2018.06.001>
- Food Standards Scotland. (2022). Shellfish results. Retrieved from <https://www.foodstandards.gov.scot/business-and-industry/industry-specific-advice/shellfish/shellfish-results>
- Gelman, A., Carlin, J., Stern, H., Dunson, D., Vehtari, A., & Rubin, D. (2014). *Bayesian data analysis, third edition (chapman and Hall/CRC texts in statistical science)* (3rd ed.). Chapman and Hall/CRC.
- Gianella, F., Burrows, M. T., Swan, S. C., Turner, A. D., & Davidson, K. (2021). Temporal and spatial patterns of harmful algae affecting Scottish shellfish aquaculture. *Frontiers in Marine Science*, 8. <https://doi.org/10.3389/fmars.2021.785174>
- Gillibrand, P. A., Siemering, B., Miller, P. I., & Davidson, K. (2016). Individual-based modelling of the development and transport of a karenia mikimotoi bloom on the north-west European continental shelf. *Harmful Algae*, 53, 118–134. <https://doi.org/10.1016/j.hal.2015.11.011>
- Glibert, P. M., Icarus Allen, J., Artioli, Y., Beusen, A., Bouwman, L., Harle, J., & Holt, J. (2014). Vulnerability of coastal ecosystems to changes in harmful algal bloom distribution in response to climate change: Projections based on model analysis. *Global Change Biology*, 20(12), 3845–3858. <https://doi.org/10.1111/gcb.12662>
- Grasso, I., Archer, S. D., Burnell, C., Tupper, B., Rauschenberg, C., Kanwit, K., & Record, N. R. (2019). The hunt for red tides: Deep learning algorithm forecasts shellfish toxicity at site scales in coastal Maine. *Ecosphere*, 10(12), e02960. <https://doi.org/10.1002/ecs2.2960>
- Hallegraeff, G. M., Anderson, D. M., Belin, C., Bottein, M.-Y. D., Bresnan, E., Chinain, M., et al. (2021). Perceived global increase in algal blooms is attributable to intensified monitoring and emerging bloom impacts. *Communications Earth & Environment*, 2(1), 117. <https://doi.org/10.1038/s43247-021-00178-8>
- Highlands and Islands Enterprise, Marine Scotland. (2017). The value of aquaculture to Scotland [Report]. <https://www.hie.co.uk/media/3035/valueplusofplusscottishplusaquacultureplus2017plus-plusreport.pdf>
- Hoagland, P., & Scatasta, S. (2006). The economic effects of harmful algal blooms. In E. Granéli & J. T. Turner (Eds.), *Ecology of harmful algae* (pp. 391–402). Springer Berlin Heidelberg. [https://doi.org/10.1007/978-3-540-32210-8\\_30](https://doi.org/10.1007/978-3-540-32210-8_30)
- Janssen, A. B. G., Janse, J. H., Beusen, A. H. W., Chang, M., Harrison, J. A., Huttunen, I., et al. (2019). How to model algal blooms in any lake on earth. *Current Opinion in Environmental Sustainability*, 36, 1–10. <https://doi.org/10.1016/j.cosust.2018.09.001>
- Kalbfleisch, J. D., & Prentice, R. L. (2002). *The statistical analysis of failure time data* (2nd ed. (2nd ed.)). Wiley. <https://doi.org/10.1002/9781118032985>
- Karasiewicz, S., Chapelle, A., Bacher, C., & Soudant, D. (2020). Harmful algae niche responses to environmental and community variation along the French coast. *Harmful Algae*, 93, 101785. <https://doi.org/10.1016/j.hal.2020.101785>
- Kudela, R. M., Anderson, C., & Ruhl, H. (2021). The California harmful algal bloom monitoring and alert program: A success story for coordinated ocean observing. *Oceanography*, 84–85. <https://doi.org/10.5670/oceanog.2021.supplement.02-30>
- Lee, J. H. W., Huang, Y., Dickman, M., & Jayawardena, A. W. (2003). Neural network modelling of coastal algal blooms. *Ecological Modelling*, 159(2), 179–201. [https://doi.org/10.1016/S0304-3800\(02\)00281-8](https://doi.org/10.1016/S0304-3800(02)00281-8)
- Lima, M., Relvas, P., & Barbosa, A. (2022). Variability patterns and phenology of harmful phytoplankton blooms off southern Portugal: Looking for region-specific environmental drivers and predictors. *Harmful Algae*, 116, 102254. <https://doi.org/10.1016/j.hal.2022.102254>
- Manfrin, C., De Moro, G., Torboli, V., Venier, P., Pallavicini, A., & Gerdol, M. (2012). Physiological and molecular responses of bivalves to toxic dinoflagellates. *Invertebrate Survival Journal*, 9(2).
- Mardones, J., Holland, D., Anderson, L., Véronique, L. B., Gianella, F., Clement, A., et al. (2020). Estimating and mitigating the economic costs of harmful algal blooms on commercial and recreational shellfish harvesters. *PICES Scientific Report*, 66–83.
- Martino, S., Gianella, F., & Davidson, K. (2020). An approach for evaluating the economic impacts of harmful algal blooms: The effects of blooms of toxic dinofysis spp. on the productivity of Scottish shellfish farms. *Harmful Algae*, 99, 101912. <https://doi.org/10.1016/j.hal.2020.101912>



- Montresor, M., & Marino, D. (1996). 03). Modulating effect of cold-dark storage on excystment in alexandrium pseudogonyaulax (dinophyceae). *Marine Biology*, 127(1), 55–60. <https://doi.org/10.1007/BF00993643>
- National Centers for Coastal Ocean Science. (2024). Lake erie harmful algal bloom forecast. Retrieved from <https://coastalscience.noaa.gov/science-areas/habs/hab-forecasts/lake-erie/>
- NOAA. (2021). National oceanographic and atmospheric administration: Gulf of Mexico harmful algal bloom forecast, tides and current. Retrieved from <https://tidesandcurrents.noaa.gov/hab/gomx.html>
- Pedersen, E. J., Miller, D. L., Simpson, G. L., & Ross, N. (2019). Hierarchical generalized additive models in ecology: An introduction with mgcv. *PeerJ*, 7, e6876. <https://doi.org/10.7717/peerj.6876>
- Pfiester, L. A., & Anderson, D. M. (1987). Dinoflagellate life-cycles and their environmental control. In F. J. R. Taylor (Ed.), *The biology of dinoflagellates* (pp. 611–648). Blackwell Scientific Publications.
- Promote Shetland. (2022). About: What drives the economy? Retrieved from <https://www.shetland.org/about>
- Reguera, B., Riobó, P., Rodríguez, F., Díaz, P. A., Pizarro, G., Paz, B., et al. (2014). Dinophysis toxins: Causative organisms, distribution and fate in shellfish. *Marine Drugs*, 12(1), 394–461. <https://doi.org/10.3390/md12010394>
- Schmidt, W., Evers-King, H. L., Campos, C. J. A., Jones, D. B., Miller, P. I., Davidson, K., & Shutler, J. D. (2018). A generic approach for the development of short-term predictions of Escherichia coli and biotoxins in shellfish. *Aquaculture Environment Interactions*, 10, 173–185. <https://doi.org/10.3354/aei00265>
- Scholin, C., Birch, J., Jensen, S., MarinIII, R., Massion, E., Pargett, D., et al. (2018). The quest to develop ecogenomic sensors: A 25-year history of the environmental sample processor (ESP) as a case study. *Oceanography*, 30(4), 100–113. <https://doi.org/10.5670/oceanog.2017.427>
- Scotland's Aquaculture. (2022). Biotxin monitoring samples [Dataset]. [http://aquaculture.scotland.gov.uk/data/biotxin\\_monitoring\\_sample.aspx](http://aquaculture.scotland.gov.uk/data/biotxin_monitoring_sample.aspx)
- Stoner, O., Economou, T., & Brown, A. R. (2022). Software and data for “A seasonal early warning framework for harmful algal blooms” [Software]. *Zenodo*. <https://doi.org/10.5281/zenodo.7248102>
- Stoner, O., Economou, T., Torres, R., Ashton, I., & Brown, A. R. (2023). Quantifying Spatio-temporal risk of harmful algal blooms and their impacts on bivalve shellfish mariculture using a data-driven modelling approach. *Harmful Algae*, 121, 102363. <https://doi.org/10.1016/j.hal.2022.102363>
- Swan, S. C., Turner, A. D., Bresnan, E., Whyte, C., Paterson, R. F., McNeill, S., et al. (2018). Dinophysis acuta in Scottish coastal waters and its influence on diarrhetic shellfish toxin profiles. *Toxins*, 10(10), 399. <https://doi.org/10.3390/toxins10100399>
- Taranu, Z. E., Gregory-Eaves, I., Steele, R. J., Beaulieu, M., & Legendre, P. (2017). Predicting microcystin concentrations in lakes and reservoirs at a continental scale: A new framework for modelling an important health risk factor. *Global Ecology and Biogeography*, 26(6), 625–637. <https://doi.org/10.1111/geb.12569>
- Trainer, V. L., Davidson, K., Wakita, K., Berdalet, E., Suddleson, M., Myre, G., & Trethewey, D. (2020). Globalhab: Evaluating, reducing and mitigating the cost of harmful algal blooms: A compendium of case studies. *PICES Press*, 28(1), 30–32.
- von Stosch, H. A. (1973). Observations on vegetative reproduction and sexual life cycles of two freshwater dinoflagellates, gymnodinium pseudopalustre schiller and woloszynskia apiculata sp. nov. *British Phycological Journal*, 8(2), 105–134. <https://doi.org/10.1080/00071617300650141>
- Weisberg, R. H., Liu, Y., Lembke, C., Hu, C., Hubbard, K., & Garrett, M. (2019). The coastal ocean circulation influence on the 2018 west Florida shelf k. brevis red tide bloom. *Journal of Geophysical Research: Oceans*, 124(4), 2501–2512. <https://doi.org/10.1029/2018JC014887>
- Wells, M. L., Karlson, B., Wulff, A., Kudela, R., Trick, C., Asnaghi, V., et al. (2020). Future HAB science: Directions and challenges in a changing climate. *Harmful Algae*, 91, 101632. <https://doi.org/10.1016/j.hal.2019.101632>
- Whyte, C., Swan, S., & Davidson, K. (2014). Changing wind patterns linked to unusually high dinophysis blooms around the Shetland Islands, Scotland. *Harmful Algae*, 39, 365–373. <https://doi.org/10.1016/j.hal.2014.09.006>
- Wood, S. N. (2011). Fast stable restricted maximum likelihood and marginal likelihood estimation of semiparametric generalized linear models. *Journal of the Royal Statistical Society*, 73(1), 3–36. <https://doi.org/10.1111/j.1467-9868.2010.00749.x>
- Wood, S. N. (2017). *Generalized additive models: An introduction with r* (2nd ed.). Chapman and Hall/CRC. <https://doi.org/10.1201/9781315370279>
- Yamahara, K. M., Preston, C. M., Birch, J., Walz, K., Marin, R., Jensen, S., et al. (2019). In situ autonomous acquisition and preservation of marine environmental dna using an autonomous underwater vehicle. *Frontiers in Marine Science*, 6(373). <https://doi.org/10.3389/fmars.2019.00373>

## References From the Supporting Information

- Wood, S. (2016). Just another Gibbs additive modeler: Interfacing jags and mgcv. *Journal of Statistical Software, Articles*, 75(7), 1–15. <https://doi.org/10.18637/jss.v075.i07>